Available online at www.sciencedirect.com
SCIENCE DIRECT®
Journal of Catalysis 227 (2004) 90–100
JOURNAL OF CATALYSIS
www.elsevier.com/locate/jcat

Selectivity-directing factors of ammonia oxidation over PGM gauzes in the Temporal Analysis of Products reactor: Primary interactions of NH_3 and O_2

J. Pérez-Ramírez [a,*], E.V. Kondratenko [b,*], V.A. Kondratenko [b], M. Baerns [b]

[a] Yara Technology Centre Porsgrunn, Catalysis and Nitric Acid Technology, PO Box 2560, N-3908, Porsgrunn, Norway
[b] Institute for Applied Chemistry Berlin-Adlershof, Richard-Willstätter-Str.12, D-12489, Berlin, Germany

Received 4 April 2004; revised 20 June 2004; accepted 26 June 2004

Abstract

The Temporal Analysis of Products (TAP) reactor has been applied to study selectivity-directing factors of the high-temperature NH_3 oxidation to NO, N_2O, and N_2 over commercial knitted Pt and woven Pt–Rh alloy gauzes at 973–1173 K. The unique features of the TAP technique enable investigation of the mechanism of this highly exothermic process under isothermal conditions over catalysts of industrial relevance, and the applicaton of much higher peak pressures as compared to surface science techniques in ultrahigh vacuum. This article focuses on the investigation of primary interactions of NH_3 and O_2. The overall reaction mechanism was found to be very similar over both Pt and Pt–Rh gauzes. NH_3 activation is favored over O_2-pretreated gauzes, while the as-received gauzes are virtually inactive for NH_3 decomposition to N_2. The selectivity to NO primarily depends on the concentration of adsorbed oxygen species. A high ratio of adsorbed O/NH_x species favors NO formation, confirming that undesirable secondary reaction paths are minimized at a high O coverage. Besides, our results suggest that the nature of oxygen species influences the distribution of NO and N_2 in the product. It is put forward that weakly bounded oxygen species lead to a high NO selectivity, while strongly bounded oxidize NH_3 into N_2. The interaction of NH_3 and NO also contributes to N_2 formation, while direct NO decomposition is practically suppressed over the oxidized gauzes. Application of isotopically labeled $^{15}NH_3$ and high peak pressures were essential for detecting N_2O formation during ammonia oxidation. Analysis of secondary interactions of NH_3 and NO in the authors' next project is required to further unravel the origins of reaction by-products like N_2O and N_2.

Keywords: NH_3 oxidation; Platinum; Rhodium; Gauze; Selectivity; NO; N_2; N_2O; Mechanism; Transient experiments; TAP reactor; Isotopes

1. Introduction

The catalytic oxidation of ammonia with air over PGM (platinum group metals) gauzes is one of the highest temperature (1073–1173 K) and shortest contact time (10^{-3}–10^{-4} s) processes in the chemical industry. The reaction is highly exothermic, yielding NO with a high selectivity (95–97%) and N_2 and N_2O as undesired by-products [1]. Academic interest lies in the challenge of elucidating details of the reaction mechanism and kinetics of product formation. However, despite numerous studies over Pt wires [2–4] and Pt single crystals [5–10], a generally accepted mechanistic description of the process at a molecular level has not yet been achieved. Early theories on the mechanism of ammonia oxidation differ in the nature of the formed intermediates, which determine a certain reaction product. Nitroxyl (HNO) [11], hydroxylamine (NH_2OH) [12], and imide (NH) [13] were postulated as possible intermediate species. Later, application of modern surface science techniques in ultrahigh vacuum (UHV) provided new insights into the reaction mechanism over single Pt crystals in a broad temperature range (300–1700 K) [5,8,9,14]. Briefly, these studies con-

---

[*] Corresponding authors.
E-mail addresses: javier.perez.ramirez@yara.com (J. Pérez-Ramírez), evgenii@aca-berlin.de (E.V. Kondratenko).

0021-9517/$ – see front matter © 2004 Elsevier Inc. All rights reserved.
doi:10.1016/j.jcat.2004.06.023

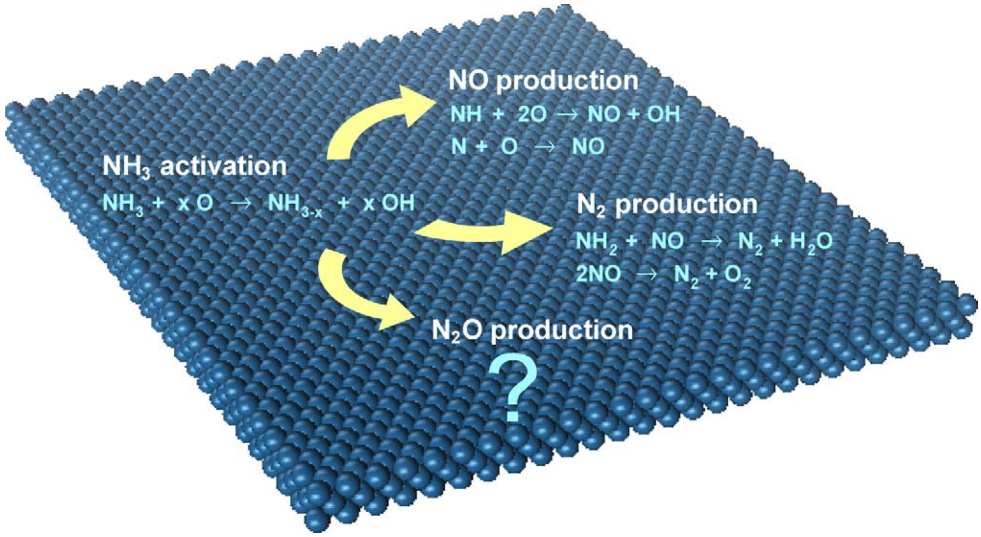

Fig. 1. Schematic impression of proposed mechanisms of product formation during ammonia oxidation on a platinum surface as derived from surface science studies in UHV (see references in text).

cluded that the oxidation of NH_3 is initiated by the formation of reactive intermediate NH_x species. Further oxidation of these ammonia fragments ultimately results in NO formation, while N_2 is formed via recombination of two nitrogen atoms or by decomposition of NO, as schematically shown in Fig. 1. Based on experiments revealing that the adsorption of ammonia is not blocked by preadsorbed oxygen, two different sites on the platinum surface have been suggested for ammonia and oxygen adsorption, on top and hollow positions, respectively [9,10,15].

Despite the valuable mechanistic information derived from UHV studies, these are carried out over model surfaces (single crystals) at extremely low partial pressures (typically 10^{-5}–10^{-7} Pa), representing a considerable gap of materials and pressure with respect to realistic industrial conditions. The robustness of this approach for achieving an accurate description of the overall mechanism can be questioned, since N_2O was never detected as a product in UHV studies and thus its formation was not discussed. Accordingly, the reaction has been considered as biphasic, yielding NO and N_2 [9]. Unquestionably, processes involving oxidation of ammonia produce N_2O as a by-product, and nitric acid production is the largest source of N_2O in the chemical industry (400 kton N_2O per year) [1]. On this basis, a proper understanding of the origin(s) of N_2O would be of great fundamental and practical relevance.

The difficulties for assessing the mechanism of the high-temperature ammonia oxidation with traditional experimental approaches at ambient pressure are principally caused by ignition of the reaction as well as by the structural and morphological changes of the metal alloy surface occurring under reaction conditions [16–18]. Kinetic instabilities have been observed over Pt wires at total pressures above 10^{-1} Pa [19–21]. Application of structured microreactors coated with Pt/Al_2O_3 has enabled kinetic data of the low-temperature ammonia oxidation to be derived [22,23]. However, these experiments were limited to 700 K and extrapolation to relevant burner temperatures is not straightforward.

In summary, two practical aspects can largely contribute to an improved mechanistic and kinetic understanding of the high-temperature ammonia oxidation: (i) isothermal conditions at typical burner temperatures and (ii) application of industrially relevant catalysts. This has been achieved by the application of a transient pulse isotopic technique, the Temporal Analysis of Products (TAP) reactor. To the best of our knowledge, no TAP studies on ammonia oxidation have been previously reported. This paper introduces the unique features of the TAP technique for the above purposes and focuses on selectivity-directing factors derived from the primary interactions between O_2 and NH_3 over commercial Pt and Pt–Rh alloy gauzes at 973–1173 K. This study is complemented by the analysis of secondary interactions of NH_3 and NO in an upcoming manuscript. Our results lead to an improved description of the mechanism(s) of product formation in ammonia burners.

2. TAP technique in NH_3 oxidation

2.1. Temperature control

Transient experiments were performed in the Temporal Analysis of Products reactor [24,25]. The gas transport in the catalytic reactor is determined by the pulse size, which can be varied in the range of 10^{13}–10^{17} molecules per pulse. In the Knudsen diffusion regime (pulse size $< 10^{15}$ molecules), purely heterogeneous steps of activation of molecules on the catalyst surface are taken into account, since any collision of molecules in the gas phase is minimized. The eventual influence of gas-phase interactions or peak pressure on a particular process can be assessed in a molecular diffusion regime (pulse size $> 10^{15}$ molecules).

A key advantage of the TAP technique over standard steady-state and unsteady-state techniques is the excellent temperature control due to the very low heat production (or consumption) associated to typical pulse sizes (0.1–10 nmol). Therefore, highly exothermic or endothermic reactions can be studied under isothermal conditions. The following estimation illustrates this unique feature for high-temperature ammonia oxidation studies. For the oxidation of 10 nmol of NH_3 to N_2 (100% conversion and selectivity) at 1073 K, an adiabatic temperature rise of ca. 2.8 K was estimated using the following expression [26]:

$$\Delta T_{\mathrm{ad}} = \frac{n \Delta H^{N_2}_{1073\ \mathrm{K}}}{m_{\mathrm{cat}} C_{\mathrm{p}}(\mathrm{Pt})}. \tag{1}$$

In this equation, n is the amount of NH_3 per pulse (10 nmol), $\Delta H^{N_2}_{1073\ K}$ is the reaction enthalpy of N_2 formation at 1073 K (-635 kJ mol^{-1}), m_{cat} is the catalyst mass (20 mg), and C_{p}(Pt) is specific heat capacity of Pt (0.133 J g^{-1} K^{-1}). The selective oxidation of ammonia to N_2O and NO would lead to a lower ΔT_{ad} due to the lower reaction enthalpies (-552 and -454 kJ mol^{-1}, respectively, at 1073 K) as compared to the oxidation to N_2. In practice, the calculated temperature rise is overestimated due to heat conduction away from the gauze. Besides, the temperature within the gauze volume is expected to be uniform due to the good heat conducting properties of platinum metal.

2.2. Peak pressure

Peak pressures in the TAP reactor can increase up to several Pa. Fig. 2 shows a simulated pressure profile during single pulsing of an inert gas like neon at 1073 K. A three-zone model considering a temperature profile in the microreactor was applied for the computation [27]. The mass transport in the microreactor is described by Ne diffusion. The highest pressure is situated at the reactor inlet for the diffusive flow. The additional peak pressure observed in the catalyst position is caused by the axial temperature gradients along the reactor. For example, if the catalyst temperature is 1073 K, the inlet and outlet temperatures of the microreactor are 340 and 380 K, respectively. Thus, the pressure gradient depends on diffusive flow and the temperature profile in the reactor. As derived from Fig. 2, the pressure in the catalyst (gauze) position increases up to 160 Pa. For a typical UHV investigation at pressures of 10^{-7} Pa, the ratio of $P_{\mathrm{UHV}}/P_{\mathrm{ambient}}$ is ca. 10^{-12}, while in the TAP reactor the ratio of $P_{\mathrm{TAP}}/P_{\mathrm{ambient}}$ is increased up to 10^{-3} (using a pulse size of 10^{16} molecules). Accordingly, the pressure gap between the TAP and the ambient pressure studies is largely reduced with respect to UHV studies.

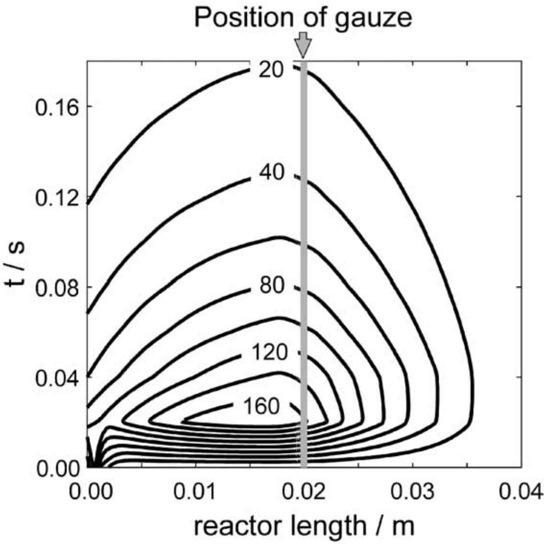

Fig. 2. Contour plot of simulated pressure profiles in the TAP microreactor during Ne pulsing at 1073 K ($D_{\mathrm{Ne}} = 1.310^{-2}$ m^2 s^{-1}, $M_{\mathrm{w}} = 20$ g mol^{-1}, pulse size $\sim 10^{16}$ molecules). The distance between two isobars is 20 Pa.

2.3. Mean residence time

For a three-zone reactor model, the mean residence time in the TAP reactor can be determined according to [28],

$$\tau^{\mathrm{dif}}_{\mathrm{res,cat}} \approx \frac{\Delta L \cdot L_{\mathrm{II}}}{D}, \tag{2}$$

where D is the gas diffusion coefficient (m^2 s^{-1}), ΔL is the gauze thickness (m), L_{II} is the length of the second inert zone (m), and $\tau^{\mathrm{dif}}_{\mathrm{res,cat}}$ is the mean residence time (s). For a pulse experiment at 1073 K with a single gauze of 0.5 mm thickness, the mean residence time was estimated to be ca. 10^{-3} s, which is comparable to typical values in industrial burners (10^{-3}–10^{-4} s).

3. Experimental

3.1. Gauze catalysts

Transient experiments were performed over two commercial PGM gauzes: (i) pure Pt, knitted pattern, Multinit type 4, supplied by Degussa, and (ii) Pt–Rh alloy, 95 wt% Pt and 5 wt% Rh, woven pattern, 1024 mesh per cm^2, supplied by K.A. Rasmussen. The wire diameter was 76 µm in both samples, as shown in Fig. 3. The SEM pictures evidence the smooth surface of the as-received samples, as expected for fresh noble metal gauzes. Due to the small amount of gases pulsed in the TAP reactor and the duration of the experiments, any surface reconstruction can be excluded in our experiments. This was confirmed by microscopy studies over the used gauzes. The typical phenomenon of sprouting or cauliflower formation in the gauze during the first days on stream in industrial burners causes dramatic increase of the surface area of the gauze, as well as changes of the surface composition [29].

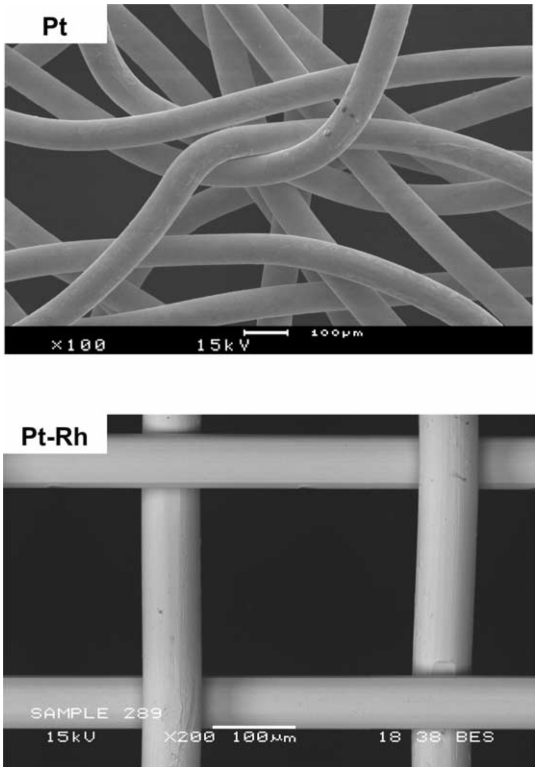

Fig. 3. Scanning electron micrographs of the knitted Pt gauze and woven Pt–Rh gauze used in this study.

3.2. TAP experiments

TAP experiments were carried out in a quartz microreactor (40 mm length and 6 mm i.d.), containing either one single piece of woven Pt–Rh gauze (25 mg) or knitted Pt gauze (110 mg), which is placed in the isothermal zone between two layers of quartz particles (sieve fraction 250–350 µm). During pulse experiments the catalyst is under vacuum conditions (10^{-5} Pa). The pulse size was varied from ca. 10^{14} to 10^{16} molecules in order to perform experiments in Knudsen and molecular diffusion regimes, respectively. The following transient experiments were performed:

- *Single pulsing of NH_3 over as-received and O_2-pretreated gauzes*. A mixture of $^{14}NH_3$:Ne = 1:1 was pulsed over the as-received gauzes in the range of 973–1173 K. The as-received gauzes were pretreated by pulsing O_2 at the corresponding reaction temperature for 2 h ($\sim$ 20 nmol of O_2 per pulse), followed by NH_3 pulsing ca. 20 s after such a treatment.
- *Single pulsing of NH_3–O_2 mixtures over O_2-pretreated gauzes*. The gauzes were pretreated in flowing O_2 at ambient pressure and 1273 K for 2 h. After evacuation, mixtures of $^{14}NH_3$:O_2:Ne = 1:2:1 or $^{15}NH_3$:O_2:Ne = 1:2:1 were pulsed in the temperature range of 973–1173 K.
- *Sequential pulsing of O_2 and NH_3 over O_2-pretreated gauzes*. The gauzes were pretreated in flowing O_2 at ambient pressure and 1273 K for 2 h. After evacuation, mixtures of O_2:Ne = 1:1 and $^{14}NH_3$:Xe = 1:1 (or $^{15}NH_3$:Xe = 1:1) were sequentially pulsed at reaction temperatures of 1023 and 1073 K using time delays of $\Delta t = 0.1$–2 s.
- *Single pulsing of NO over fresh, H_2-pretreated, and O_2-pretreated gauzes*. The gauzes were pretreated in flowing pure O_2 or H_2 at ambient pressure and 1273 K for 2 h. After evacuation, a mixture of NO:Ne = 1:1 was pulsed over the catalyst at 973–1173 K.

In the experiments, Ne (4.5), Xe (4.0), O_2 (4.5), NO (2.5), $^{14}NH_3$ (2.5), and $^{15}NH_3$ (99.9% atoms of ^{15}N) were used without additional purification. Isotopically labeled ammonia was purchased from ISOTEC. Transient responses were monitored at atomic mass units (AMUs) related to reactants, reaction products, and inert gases at the reactor outlet using a quadruple mass spectrometer (Hiden Analytical). The following AMUs were analyzed: 132 (Xe), 46 (NO_2, $^{15}N_2O$), 45 ($^{15}N^{14}NO$), 44 (N_2O, CO_2), 32 (O_2), 31 (^{15}NO, HNO), 30 (N_2O, NO, $^{15}N_2$), 29 ($^{15}N^{14}N$), 28 (N_2O, N_2), 20 (Ne), 18 (H_2O, $^{15}NH_3$), 17 (NH_3, OH), 16 (O_2, NH_3), 15 (NH_3), and 2 (H_2). For each AMU, pulses were repeated 10 times and averaged to improve the signal-to-noise ratio. The concentration of feed components and reaction products was determined from the respective AMUs using standard fragmentation patterns and sensitivity factors. The transient responses were typically normalized for a better comparison of pulse shapes.

4. Results

4.1. Single pulsing of NH_3 in Knudsen diffusion regime

The interaction of ammonia with the as-received and O_2-pretretated Pt and Pt–Rh gauzes was studied by single pulsing of ammonia in a Knudsen diffusion regime at different temperatures. No difference in ammonia conversion and products concentration was observed with the number of pulses, indicating that the gauze performance did not change during the TAP experiments. As shown in Fig. 4, the degree of ammonia conversion is very low upon NH_3 pulsing over the as-received Pt and Pt–Rh gauzes, revealing the inactivity of essentially reduced noble metal surfaces for ammonia decomposition at the short residence times in the TAP reactor. Contrarily, significant amounts of N_2, H_2, and H_2O were produced when ammonia was pulsed over the O_2-pretreated gauzes (Table 1). As shown in Fig. 4, the NH_3 conversion is in the range of 30–40%. The observed decrease in N_2 formation with an increased temperature can be associated to a decreased oxygen coverage. Our results suggest that the O_2 pretreatment results in the formation of oxygen species that are essential for ammonia activation. Desorption of such oxygen species can be assumed to increase with an increase in temperature. It should be stressed that in these experi-

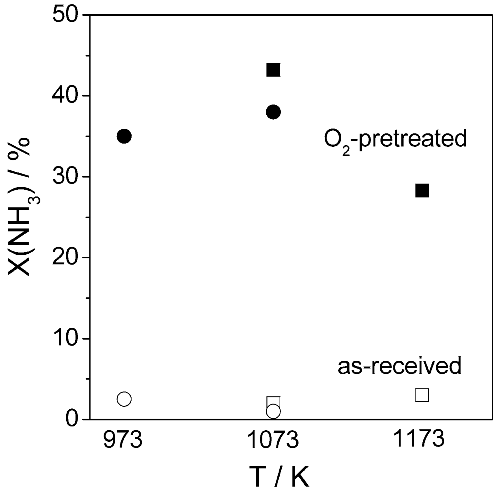

Fig. 4. Influence of catalyst pretreatment on the NH_3 conversion during single pulsing of NH_3:Ne = 1:1 over Pt (circles) and Pt–Rh (square) gauzes. Open symbols: as-received (nonpretreated) gauzes; solid symbols: O_2-pretreated gauzes. Pulse size of $NH_3 \sim 10^{14}$ molecules.

Table 1

Performance of oxygen-pretreated noble metal gauzes in ammonia decomposition in the TAP reactor

Sample	T (K)	$Y(N_2)$ (%)	Y(NO) (%)	$Y(H_2)$ (%)	$Y(H_2O)$ (%)
Pt	973	33	–	33	5.8
	1073	30	–	25	4
Pt–Rh	1073	47	–	21	25
	1173	33	0.02	21	14

Conditions: single pulsing of NH_3:Ne = 1:1; NH_3 pulse size $\sim 10^{14}$ molecules.

ments, NH_3 pulses were introduced in the TAP reactor 20 s after the O_2 pretreatment was finalized. This relatively long time suggests that stable surface oxygen species deposited by pulsing O_2 over the as-received gauzes are responsible for NH_3 conversion into N_2, H_2, and H_2O formation. As shown in Table 1, hydrogen is obtained in excess water over Pt gauze ($H_2/H_2O \sim 6$), while a ratio of $H_2/H_2O \sim 1$ was achieved over Pt–Rh gauze. This can be attributed to the presence of rhodium in the latter catalyst, which has a higher affinity for oxygen than platinum. The higher degree of oxidation of Pt–Rh gauze as compared to Pt gauze may induce a more extended oxidation of H-containing species on the catalyst surface leading to H_2O. Only traces of NO were observed over Pt–Rh gauze at 1173 K (Table 1). The insignificant amount of NO produced in these experiments can be attributed to the low concentration of oxygen species on the catalyst surface (O coverage). However, it cannot be totally excluded that long-living, strongly bounded oxygen species are able to dehydrogenate ammonia but not transferable into the corresponding ammonia intermediate to yield NO, with the subsequent N_2 production. A more detailed analysis on the effect of concentration and nature of O species on the products distribution is provided in Sections 4.2 and 5.1.

4.2. *Interaction of O_2 and NH_3 in the Knudsen diffusion regime*

In order to derive mechanistic insights into product formation of ammonia oxidation over Pt and Pt–Rh gauzes, primary interactions of O_2 and NH_3 were investigated in sequential pulse experiments at time delays in the range of 0–2 s. This contrasts with the longer period of 20 s between the last oxygen pulse and the first ammonia pulse in the experiments described in Section 4.1, and enables an analysis of the effect of the concentration and the nature of O-adsorbed species formed during the first O_2 pulse (pump) on NH_3 activation in the second pulse (probe). Fig. 5 shows the transient responses resulting from sequential pulsing of oxygen (O_2:Ne = 1:1) and ammonia ($^{14}NH_3$:Xe = 1:1) at $\Delta t = 0.2$ s for Pt gauze and $\Delta t = 0.5$ s for Pt–Rh gauze. N_2, NO, H_2O, and H_2 were the only reaction products detected in ammonia pulse, while no products were observed in the oxygen pulse. Accordingly, no N-containing species, which can be eventually oxidized in the O_2 pulse, were stabilized on the catalyst surface. The transient responses of the different species over Pt and Pt–Rh gauzes were very similar, suggesting a minor influence of the gauze composition on the intrinsic mechanism of primary NH_3–O_2 interactions.

The O_2 transient response clearly shows that the concentration of gas-phase oxygen sharply decreases upon NH_3 pulsing (Fig. 5). This sharp decrease in the oxygen signal indicates that adsorbed oxygen species rapidly react with NH_3. For both Pt and Pt–Rh gauzes, NO appears directly at the time of the ammonia pulse, indicating its formation directly from ammonia. The transient response of NO is sharper and appears at shorter times than the transient response of N_2 (Fig. 5). This suggests that the primarily formed NO is transformed into N_2 via a secondary reaction with NH_3. This aspect will be further analyzed upon investigation of NO and NH_3 interactions in an upcoming manuscript.

The NO yield and NH_3 conversion vs. time delay in O_2–NH_3 sequential pulse experiments at 1073 K are shown in Fig. 6. NO yields close to 70% with a degree of NH_3 conversion above 80% were obtained when a mixture of O_2:NH_3:Ne = 2:1:1 was pulsed (equivalent to $\Delta t = 0$ s) over the gauzes. The NO yield over Pt and Pt–Rh gauzes strongly decreased upon increasing the time delay, being ca. 1% at $\Delta t = 0.1$ s. However, the NH_3 conversion remained practically unchanged in the range $\Delta t = 0$–2 s, indicating a complete selectivity towards N_2, as observed during single pulsing of NH_3 over the O_2-pretreated gauzes at a somewhat lower degree of ammonia conversion (ca. 40%, see Fig. 4). The result in Fig. 6 strongly suggests the importance not only of the oxygen coverage but also of the nature of the adsorbed oxygen species on the selectivity of NH_3 oxidation to NO.

Finally, a very weak and broad signal at AMU 44 was observed during sequential pulse experiments over Pt and

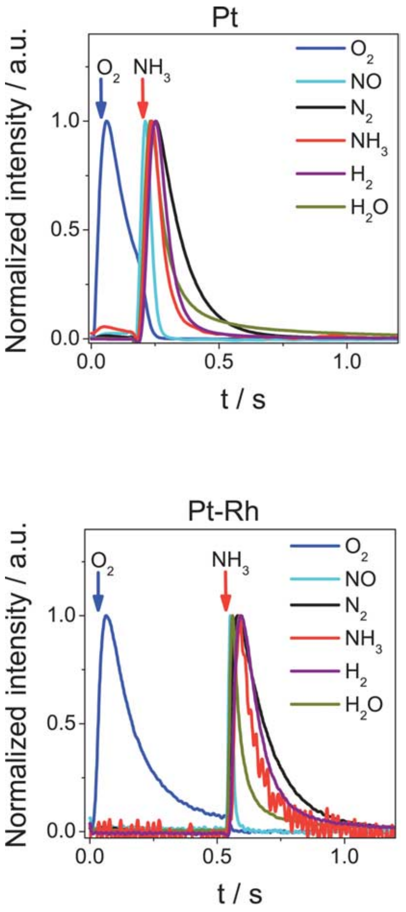

Fig. 5. Transient responses during sequential pulsing of O_2:Ne = 1:1 and NH_3:Xe = 1:1 over Pt and Pt–Rh gauzes at 1073 K. Pulse sizes of O_2 and NH_3 ~ 10^{14} molecules.

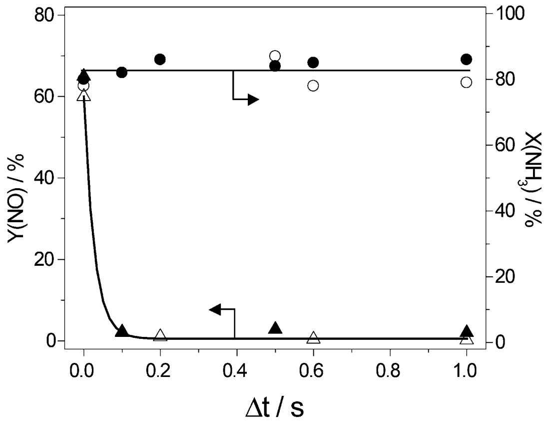

Fig. 6. NO yield (triangles) and NH_3 conversion (circles) over Pt (open symbols) and Pt–Rh (solid symbols) gauzes vs. time delay between O_2 and NH_3 in sequential pulse experiments at 1073 K. Pulse sizes of O_2 and NH_3 ~ 10^{14} molecules.

Table 2
Performance of noble metal gauzes and SiO_2 spheres in NH_3 oxidation in the TAP reactor

Sample	T (K)	Diffusion regime	$X(^{15}NH_3)$ (%)	$Y(^{15}NO)$ (%)
Pt gauze	1023	Knudsen	92	55
		Molecular	91	61
	1073	Knudsen	90	56
		Molecular	92	62
Pt–Rh gauze	1023	Knudsen	87	57
		Molecular	87	59
	1073	Knudsen	90	61
		Molecular	86	58
SiO_2 spheres	1023	Molecular	7	1.6
	1073	Molecular	9	2.2

Conditions: single pulsing of a mixture $^{15}NH_3$:O_2:Ne = 1:2:1; $^{15}NH_3$ pulse size ~ 10^{14} molecules (Knudsen diffusion regime) and ~ 10^{16} molecules (molecular diffusion regime).

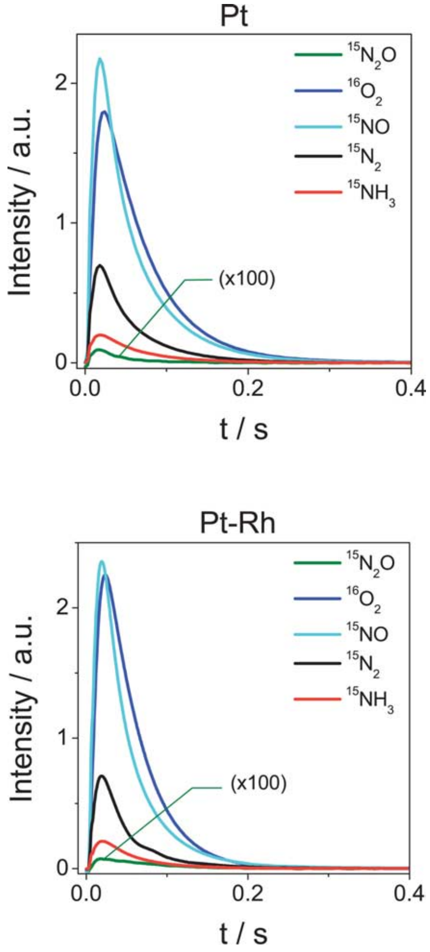

Fig. 7. Transient responses during single pulsing of an ammonia–oxygen mixture ($^{15}NH_3$:O_2:Ne = 1:2:1) over Pt and Pt–Rh gauzes at 1073 K. Pulse size of $^{15}NH_3$ ~ 10^{16} molecules.

Pt–Rh gauzes (not shown in Fig. 5). This cannot be unambiguously attributed to N_2O, since the mass also corresponds to CO_2. It is well known that the surface of commercial noble metal gauzes is covered by substantial amounts of carbon [30]. These carbon deposits can be oxidized to CO_2 during O_2 pulsing in the TAP reactor at the high temperatures investigated. Discrimination between N_2O and CO_2 in mass spectrometry has been achieved by application of isotopically labeled $^{15}NH_3$ instead of the nonlabeled $^{14}NH_3$, as described in Section 4.3.

4.3. Interaction of O_2 and NH_3 in the molecular diffusion regime

^{15}NO was the main N product upon pulsing of a mixture of $^{15}NH_3:O_2:Ne = 1:2:1$ over the Pt and Pt–Rh gauzes, with a yield $> 55\ \%$ (Table 2 and Fig. 7). As shown in Table 2, the activity of inert SiO_2 spheres is very low, revealing the negligible contribution of gas-phase reactions under the applied conditions in the TAP reactor. No dependence was found between the yield of NO and the diffusion regime, i.e., Knudsen or molecular diffusion. This further supports that NO formation purely stems from heterogeneous processes occurring at the catalyst surface.

A relevant aspect of the experiments with $^{15}NH_3$ under molecular diffusion regime is the detection of nitrous oxide as a reaction product ($^{15}N_2O$ in Fig. 7). Isotopically labeled $^{15}NH_3$ was used to discriminate between eventual formation of $^{15}N_2O$ (AMU 46) and the always present background signal of CO_2 (AMU 44). Fig. 8 shows the vital importance of the pulse size and the application of the N-labeled ammonia isotope in the TAP experiments to obtain, for the first time, relevant mechanistic information about N_2O formation during the high-temperature ammonia oxidation over PGM gauzes. The figure shows the transient responses of $^{15}N_2O$ and the signal with AMU 44 (mainly CO_2) when a mixture of $^{15}NH_3:O_2:Ne = 1:2:1$ was pulsed over the Pt and Pt–Rh gauzes at 1073 K in Knudsen and molecular diffusion regimes. The formation of nitrous oxide during ammonia oxidation is a function of the peak pressure in the TAP reactor. $^{15}N_2O$ was never detected when small pulses of the ammonia–oxygen mixture were applied (in the Knudsen diffusion regime), while a weak signal at AMU 44 can be observed. Contrarily, $^{15}N_2O$ is clearly observed when the pulse size was increased in the molecular diffusion regime. For both samples, the transient response of CO_2 with AMU 44 is more intense and broader. Accordingly, the amount of CO_2 derived from carbon impurities in the commercial gauzes (even after pretreatment in pure O_2 at 1273 K) is sufficient to mask the signal corresponding to N_2O, although both CO_2 and N_2O can be nicely uncoupled in mass spectrometry if isotopically labeled ammonia is applied.

Blank experiments in the TAP microreactor filled with quartz particles were carried out in order to exclude N_2O formation as a consequence of a homogeneous process or related to the reactor walls. The amount of N_2O formed in these experiments was 5 times lower N_2O as compared to experiments with the gauzes in Fig. 7. Accordingly, it can concluded that the formation of N_2O is a consequence

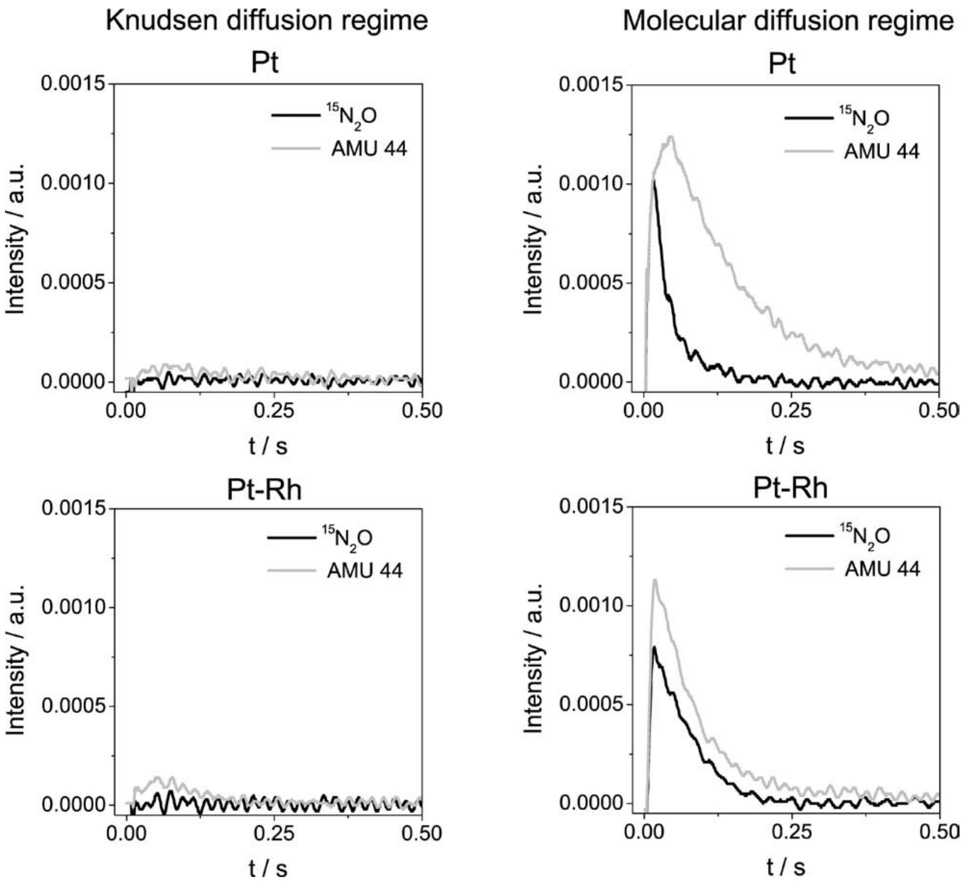

Fig. 8. Transient responses of $^{15}N_2O$ and the signal with AMU 44 during single pulsing of an ammonia–oxygen mixture ($^{15}NH_3:O_2:Ne = 1:2:1$) over Pt and Pt–Rh gauzes at 1073 K. Pulse sizes of $^{15}NH_3$ were $\sim 10^{14}$ and $\sim 10^{16}$ molecules in Knudsen and molecular diffusion regimes, respectively.

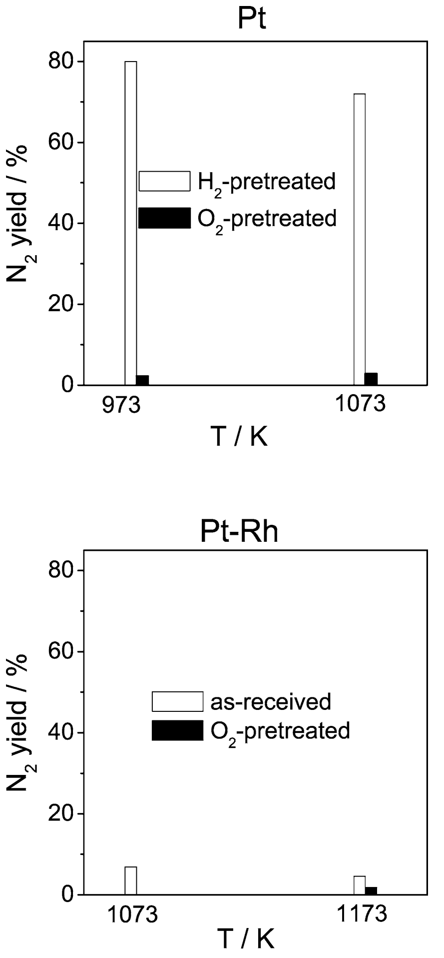

Fig. 9. N_2 yield upon single pulsing of NO:Ne = 1:1 over as-received and pretreated Pt and Pt–Rh gauzes. Pulse size of NO $\sim 10^{14}$ molecules.

of a heterogeneous process and the no observation in the Knudsen regime can be related to the detection limit of the analytical unit in relation to the low amount of N_2O formed.

4.4. Single pulsing of NO

Contrary to the results of single NH_3 pulse experiments in Section 4.1, the as-received or H_2-pretreated gauzes show a significant activity toward direct NO decomposition to N_2 and O_2 at 973–1173 K (Fig. 9). The N_2 yield is significantly higher over the H_2-pretreated gauze, indicating the affinity of NO for the reduced noble metal surface, in agreement with previous NO dissociation studies over a clean Pt(100) single crystal [9,31]. N_2O was not observed as a reaction product in the temperature range investigated. NO decomposition over Pt and Pt–Rh gauzes was nearly suppressed in the presence of adsorbed oxygen species in view of the very low NO conversion over the O_2-pretreated gauzes (Fig. 9). Thus, the gauze activity for direct NO decomposition is a function of the degree of oxidation of the catalyst surface.

5. Discussion

5.1. Primary interactions of ammonia and oxygen

The low activity of the as-received Pt and Pt–Rh gauzes for ammonia decomposition at high temperatures (see Table 1 and Fig. 1) is in good agreement with a previous study by Bradley et al. [10] using molecular beams under UHV at temperatures up to 400 K. These authors concluded that NH_3 did not dissociate over a hex-R Pt surface, while the reaction proceeds very slowly over a clean (1 × 1) Pt surface. In contrast with these results, Schmidt and coworkers [32–34] determined the kinetics of ammonia decomposition over different Pt specimens in the temperature range of 500–1400 K, obtaining the following activity order: polycrystalline $>$ (210) $>$ (110) $>$ (100)-hex $>$ (111). The ability of polycrystalline Pt to dissociate ammonia was found to be one order of magnitude higher than that of Pt(111). This apparent controversy can be explained if taking into account that the works by Schmidt and co-workers involved pretreatment of the Pt catalysts in an oxygen flow. As we have demonstrated, the oxygen species formed during O_2 pretreatement are responsible for ammonia decomposition. In addition, the residence time in the TAP reactor was 10^4–10^5 times shorters than that applied in [34]. Accordingly, a very slow ammonia activation process on essentially reduced metal sites cannot be detected under TAP conditions. Single pulsing of NH_3 over the O_2-pretreated Pt and Pt–Rh gauzes leads to considerable amounts of N_2, H_2, and H_2O. This is also consistent with UHV studies on Pt(100) [10], further supporting that adsorbed oxygen species dramatically enhance NH_3 activation.

The formation of H_2O and N_2 in our experiments can be explained by the simplified reaction scheme in Eqs. (3)–(8). First, gas-phase oxygen and ammonia adsorb over an active site, denoted as “s” [Eqs. (3) and (4)]. Based on low-temperature UHV studies, a dual-site model has been postulated for NH_3 oxidation over platinum, where ammonia and oxygen adsorb on on-top and hollow sites, respectively [9,10,15,23]. Since, no experimental evidence to support this model can be derived from our experiments, one common adsorption site for both species has been considered. The primary step of ammonia decomposition is H stripping from NH_3 by adsorbed atomic oxygen species leading to NH_2 and OH fragments [Eq. (5)]. NH_2 fragments can be further dehydrogenated by adsorbed oxygen species (or hydroxyl groups) according to Eqs. (5)–(9). Recombination of two surface nitrogen atoms [Eq. (10)] will ultimately result in N_2 formation [8–10,14].

$$\mathrm{NH_3 + s \longrightarrow s\text{–}NH_3}, \tag{3}$$

$$\mathrm{O_2 + 2s \longrightarrow 2s\text{–}O}, \tag{4}$$

$$\mathrm{s\text{–}NH_3 + s\text{–}O \longrightarrow s\text{–}NH_2 + s\text{–}OH}, \tag{5}$$

$$\mathrm{s\text{–}NH_2 + s\text{–}O \longrightarrow s\text{–}NH + s\text{–}OH}, \tag{6}$$

$$\mathrm{s\text{–}NH + s\text{–}O \longrightarrow s\text{–}N + s\text{–}OH}, \tag{7}$$

$$\text{s–NH}_2 + \text{s–OH} \longrightarrow \text{s–NH} + \text{s} + H_2O, \tag{8}$$

$$\text{s–NH} + \text{s–OH} \longrightarrow \text{s–N} + \text{s} + H_2O, \tag{9}$$

$$\text{s–N} + \text{s–N} \longrightarrow N_2 + 2\text{s}. \tag{10}$$

The formation of hydrogen during single pulsing of NH_3 (Sections 4.1 and 4.2) suggest a relatively low oxygen coverage of the surface as compared to the amount of ammonia pulsed. Based on this, several additional reaction routes for N_2 and H_2 formation can be suggested in Eqs. (11)–(14), which should be favored in the presence of excess ammonia.

$$\text{s–NH}_x + \text{s–NH}_x \longrightarrow N_2 + xH_2, \tag{11}$$

$$\text{s–NH}_2 + \text{s} \longrightarrow \text{s–NH} + \text{s–H}, \tag{12}$$

$$\text{s–NH} + \text{s} \longrightarrow \text{s–N} + \text{s–H}, \tag{13}$$

$$\text{s–H} + \text{s–H} \longrightarrow H_2 + 2\text{s}. \tag{14}$$

However, hydrogen was not observed upon pulsing of a mixture of oxygen and ammonia over the Pt and Pt–Rh gauzes, water being the only H-containing reaction product. In these experiments, a high yield of NO was achieved (Fig. 6). From these results, it can be concluded that the selectivity of NH_3 oxidation toward NO formation is increased when the concentration of surface oxygen species (O coverage) is sufficiently high for striping all H atoms from NH_3 and for further oxidation of the resulting NH_x ($x < 3$) intermediates to NO [Eq. (15)]. The structure of the preferred NH_x intermediate has been subject of controversy and remains unsolved.

$$\text{s–NH}_x + n\text{s–O} \longrightarrow \text{NO} + \text{s–H}_x\text{O} + (n-1)\text{s}. \tag{15}$$

At low O coverages, the relative concentration of surface NH_x species should be obviously higher than the concentration of surface O species. Therefore, recombination of two highly reactive NH_x fragments will prevail over the oxidation process in Eq. (15). Contrarily, intermediate NH_x species will be entrapped by oxygen species at high O coverages, favoring the pathway toward NO formation.

Nonetheless, from the results of single pulsing of NH_3 over the O_2-pretreated gauzes and sequential pulsing of O_2 and NH_3 at different time delays, it can be put forward that not only the O coverage is essential for a high NO selectivity, but also the nature of the adsorbed oxygen species. In single ammonia pulsing over the oxidized gauzes, no NO was detected, while the degree of NH_3 conversion to N_2 was substantial (ca. 40%). A certain NO yield was observed in sequential pulsing of oxygen and ammonia with $\Delta t = 0.2$ or 0.5 s, but not comparable to that obtained upon pulsing NH_3–O_2 mixtures (e.g., 1% vs 70% over Pt–Rh gauze at 1073 K, see Fig. 6). Still, the degree of NH_3 conversion at different time delays in the range $\Delta t = 0$–2 s was very similar (ca. 80%). Based on these data, we tentatively propose that strongly bounded oxygen species, which stay on the catalyst surface after the O_2 pretreatment, catalyze NH_3 activation. However in view of the high N_2 selectivity, the stability of the O species on the metal should be such that the recombination of dehydrogenated NH_x fragments is much more favorable that the O transfer into NH_x to form NO. We can exclude direct NO decomposition as a possible reaction route for the high N_2 production, since this process is suppressed over O_2-pretreated Pt surfaces (see Section 4.4).

In a simplistic way, Fig. 10 illustrates the proposed effect of the coverage and nature of adsorbed O species on the NO and N_2 selectivity during the high-temperature NH_3 oxidation over PGM gauzes. Two different pools of adsorbed oxygen species can be considered, which are characterized by strong (O) or weak (O*) binding to the metal on the catalyst surface. Strongly bounded O species are active for NH_3 activation [Eqs. (5)–(7)], leading to N_2, H_2O, and H_2. Based on these results, water formation [Eqs. (8) and (9)] is believed to be energetically favorable in comparison with removal of the strongly bounded oxygen by ammonia fragments resulting in NO formation. Therefore, a high NO selectivity requires not only an optimal (high) ratio of O/NH_x on the catalyst surface, but also the presence of short-living and highly mobile oxygen species.

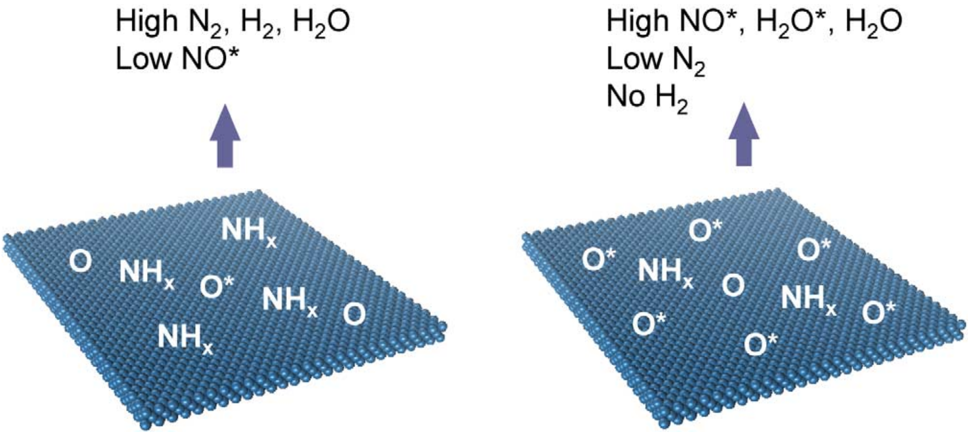

Fig. 10. Influence of the oxygen coverage and the nature of adsorbed oxygen species on the product distribution during NH_3 oxidation. O and O* denote strongly bounded and weakly bounded oxygen species, respectively.

5.2. *Products formation in ammonia oxidation*

The shape of the transient responses of NO during O_2–NH_3 interactions in sequential pulse experiments (Fig. 5) clearly indicates that NO is a primary product of the high-temperature reaction between surface NH_x and O species over Pt and Pt–Rh gauzes. The yield of NO was very similar in Knudsen and molecular diffusion regimes (Table 2), which further supports that gas-phase reactions play no role in NO formation under the transient vacuum conditions of the TAP reactor.

With respect to N_2 formation, several reaction pathways can be discussed. Apart from the recombination of NH_x fragments [Eq. (11)] at low O/NH_x ratios (low O coverage or excess of NH_3) or in the presence of strongly bounded O species (see Fig. 10), two other processes should be considered: (i) NO decomposition and (ii) a secondary process involving NH_3 and NO. Single pulsing of NO in Fig. 9 and previous studies [9,31] have shown the high affinity of reduced noble metal surfaces for NO decomposition to N_2 [Eq. (16)], with no formation of N_2O. However, this pathway is practically suppressed over oxidized noble metal surfaces, thus having an insignificant contribution in NH_3 oxidation under excess of O_2.

Sequential pulsing experiments of O_2 and NH_3 in Fig. 5 have shown a very fast reaction of the formed NO at the time of the NH_3 pulse. As a result, the NO pulse strongly decreases and a broad N_2 transient response is obtained. These results strongly suggest that the reduction of NO with adsorbed NH_x species [Eq. (17)] is a major pathway to N_2 in ammonia burners, as concluded from UHV studies [9,10]. Selectivity-directing factors toward N_2 formation will be further assessed in an upcoming manuscript.

$$2\mathrm{NO} + 2\mathrm{s} \longrightarrow \mathrm{N_2} + \mathrm{s{-}O} + \mathrm{s}, \tag{16}$$

$$\mathrm{s{-}NH}_x + \mathrm{NO} \longrightarrow \mathrm{N_2} + \mathrm{s{-}H}_x\mathrm{O}. \tag{17}$$

Finally, the formation of N_2O during NH_3 oxidation should be discussed. As noted in the Introduction, N_2O was never detected as a product during NH_3 oxidation over Pt single crystals in surface science studies under UHV conditions. Overcoming this limitation, our TAP study has demonstrated N_2O formation when a mixture of oxygen and ammonia was pulsed over Pt and Pt–Rh gauzes in a molecular diffusion regime. The amount of N_2O formed is very small, not being detected during ammonia oxidation in a Knudsen diffusion regime, i.e., at low peak pressures. Associated with the low N_2O concentrations, it should be stressed that the application of isotopically labeled ammonia ($^{15}NH_3$) was essential in order to uncouple the analysis of N_2O and CO_2 (due to carbon impurities on the gauze surface) in mass spectrometry. The small amounts of N_2O formed suggest that the contribution of NH_3 oxidation toward this product is negligible. In fact, a recent TAP study has proven N_2O results from the reaction between adsorbed ammonia intermediates and nitric oxide over Pt–Rh gauze [35]. Therefore it can be expected that the rate of N_2O formation is a stronger function of NH_3 and NO partial pressures as compared to those of NO and N_2 formation. As a consequence, the extremely low reactant peak pressures (1–5 Pa) in a Knudsen diffusion regime are apparently suitable for a proper formation of NO and N_2 but insufficient for N_2O. At the investigated temperatures in the TAP reactor, N_2O is the N-containing product formed in the lowest concentration, which is also the case in industrial ammonia burners [1]. This reasoning can also explain the no identification of N_2O as a reaction product in surface science studies under ultrahigh vacuum conditions. As noted in Section 2.2, the peak pressure in the TAP reactor for a pulse size of 10^{16} molecules is considerably higher (ca. 10^9 times) than in UHV. Furthermore, these investigations have been carried out with nonisotopically labeled ammonia, which makes it impossible to accurately determine the small amounts of N_2O formed.

6. Conclusions

The TAP technique offers unique features for investigating the mechanism and kinetics of the high-temperature ammonia oxidation:

- With respect to steady-state techniques, the excellent control of temperature due to the low amount of gases pulsed (0.1–10 nmol), as well as the minor influence of homogeneous processes and wall effects;
- With respect to surface science techniques in UHV, the use of catalytic surfaces of industrial relevance and the operation at a much higher peak pressure.

The following mechanistic aspects have been elucidated from the investigation of primary NH_3–O_2 interactions over commercial Pt and Pt–Rh gauzes at 973–1173 K:

- Overall, the mechanism of NH_3 oxidation was found to be very similar over gauzes having different composition (Pt or Pt–Rh) and geometry (knitted or woven).
- NH_3 activation requires the presence of adsorbed oxygen species on the catalyst surface. Reduced metal surfaces show no activity for ammonia decomposition.
- NO is a primary product of NH_3 oxidation and its selectivity is favored at high O coverage. Nonetheless, the nature of oxygen species is also suggested to influence the product distribution of NO and N_2. Strongly bounded oxygen species activate ammonia and lead to a high N_2 selectivity by recombination of NH_x species. On the contrary, weakly bounded oxygen species are effectively transferred into the NH_x intermediates yielding NO. Accordingly, the highest NO yield is achieved when NH_3 and O_2 are simultaneously pulsed over the Pt and Pt–Rh gauzes.
- The selectivity toward NO does not strongly depend on the diffusion regime (Knudsen or molecular), indicating

that the desired product in the high-temperature ammonia oxidation originates from purely heterogeneous processes.
- Apart from the recombination of NH_x fragments at low surface O/NH_x ratios as the source of N_2, it can be concluded that N_2 also originates from the secondary reaction of NH_3 and NO.
- Direct decomposition of NO into N_2 and O_2 effectively occurs over the reduced gauzes, but is practically suppressed in the presence of adsorbed oxygen species.
- Small amounts of N_2O were detected upon pulsing of ammonia–oxygen mixtures over Pt and Pt–Rh gauzes. To this end, the use of isotopically labeled $^{15}NH_3$ and high peak pressures (molecular diffusion regime) are required. Blank experiments confirmed that N_2O formation stems from a heterogeneous process. The no observation of N_2O during ammonia oxidation under the Knudsen diffusion regime and in previous UHV studies is related to the detection limit of the analysis.

Acknowledgments

Yara International ASA is acknowledged for financial support and for permission to publish the results with Pt–Rh gauze. V.A.K. and M.B. are thankful for financial support from the Deutsche Forschungsgemeinschaft (DFG) in the frame of the competence network “Bridging the gap between real and ideal systems in heterogeneous catalysis SPP 1091.” The authors are indebted to L. Mader for technical assistance in the TAP experiments.

References

[1] J. Pérez-Ramírez, F. Kapteijn, K. Schöffel, J.A. Moulijn, Appl. Catal. B 44 (2003) 117.
[2] Y.M. Fogel, B.T. Nadytko, V.F. Rybalko, V.I. Shvachko, I.E. Korobchanskaya, Kin. Katal. 5 (1964) 496.
[3] C.W. Nutt, S.W. Karup, Nature 224 (1969) 169.
[4] T. Pignet, L.D. Schmidt, J. Catal. 40 (1975) 212.
[5] J.L. Gland, V.N. Korchak, J. Catal. 53 (1978) 9.
[6] J.L. Gland, G.C. Woodward, J. Catal. 61 (1980) 543.
[7] M. Asscher, W.L. Guthrie, T.-H. Lin, G.A. Somorjai, J. Phys. Chem. 88 (1984) 3233.
[8] W.D. Mieher, W. Ho, Surf. Sci. 322 (1995) 151.
[9] J.M. Bradley, A. Hopkinson, D.A. King, J. Phys. Chem. 99 (1995) 17032.
[10] J.M. Bradley, A. Hopkinson, D.A. King, Surf. Sci. 371 (1997) 255.
[11] L. Andrussow, Z. Angew. Chem. 39 (1926) 321.
[12] M. Bodenstein, Z. Elektrochem. 41 (1935) 466.
[13] F. Raschig, Z. Angew. Chem. 40 (1927) 1183.
[14] M. Kim, S.J. Pratt, D.A. King, J. Am. Chem. Soc. 122 (2000) 2409.
[15] N. Materer, U. Starke, A. Barbieri, R. Döll, K. Heinz, M.A. Van Hove, G.A. Somorjai, Surf. Sci. 325 (1995) 207.
[16] R.W. McCabe, T. Pignet, L.D. Schmidt, J. Catal. 32 (1974) 114.
[17] M. Flytzani-Stephanopoulos, S. Wong, L.D. Schmidt, J. Catal. 49 (1977) 51.
[18] M.R. Luibovskii, V.V. Barelko, Kinet. Katal. 35 (1994) 412.
[19] M. Sheituch, L.D. Schmidt, J. Phys. Chem. 92 (1988) 3404.
[20] L. Lobban, G. Philippou, D. Luss, J. Phys. Chem. 93 (1989) 733.
[21] G. Philippou, D. Luss, Chem. Eng. Sci. 48 (1993) 2313.
[22] E.V. Rebrov, M.H.J.M. de Croon, J.C. Schouten, Catal. Today 69 (2001) 183.
[23] E.V. Rebrov, M.H.J.M. de Croon, J.C. Schouten, Chem. Eng. J. 90 (2002) 61.
[24] J.T. Gleaves, J.R. Ebner, T.C. Kuechler, Catal. Rev.-Sci. Eng. 30 (1988) 49.
[25] J.T. Gleaves, G.S. Yablonsky, P. Phanawadee, Y. Schuurman, Appl. Catal. A 160 (1997) 55.
[26] O. Levenspiel, in: Chemical Reaction Engineering, Wiley, New York, 1999, p. 668.
[27] M. Soick, D. Wolf, M. Baerns, Chem. Eng. Sci. 55 (2000) 2875.
[28] S.O. Shekhtman, G.S. Yablonsky, S. Chen, J.T. Gleaves, Chem. Eng. Sci. 54 (1999) 4371.
[29] R.J. Farrauto, C.H. Bartholomew, in: Fundamentals of Industrial Catalytic Processes, Chapman & Hall, London, 1997, p. 481.
[30] P.A. Kozub, G.I. Gryn, I.I. Goncharov, Platinum Metals Rev. 44 (2000) 77.
[31] R.J. Gorte, L.D. Schmidt, J.L. Gland, Surf. Sci. 109 (1981) 367.
[32] D.G. Löffler, L.D. Schmidt, J. Catal. 41 (1976) 440.
[33] D.G. Löffler, L.D. Schmidt, Surf. Sci. 59 (1976) 195.
[34] G.A. Papapolymerou, L.D. Schmidt, Langmuir 1 (1985) 488.
[35] J. Pérez-Ramírez, E.V. Kondratenko, Chem. Commun. (2004) 376.